NASA TECHNICAL MEMORANDUM

NASA TM X-71665

NASA TM X-71665

MEASUREMENT OF SPUTTERED EFFLUX FROM 5-, 8-, AND 30-CM DIAMETER MERCURY ION THRUSTERS

by A. J. Weigand and M. J. Mirtich
Lewis Research Center
Cleveland, Ohio 44135

TECHNICAL PAPER to be presented at
Eleventh Electric Propulsion Conference sponsored
by American Institute of Aeronautics and Astronautics
New Orleans, Louisiana, March 19-21, 1975

MEASUREMENT OF SPUTTERED EFFLUX FROM 5-, 8-, AND 30-CM DIAMETER MERCURY ION THRUSTERS

A. J. Weigand and M. J. Mirtich
Lewis Research Center
National Aeronautics and Space Administration
Cleveland, Ohio

Abstract

A study was undertaken to investigate the sputtered efflux from 5-, 8-, and 30-cm diameter mercury ion thrusters. Quartz crystal microbalances and fused silica samples were used to analyze the sputtered flux. Spectral transmittance measurements and spectrographic analysis of the samples were made after they were exposed to different thruster effluence by operating the thrusters at various conditions and durations of time. These measurements were used to locate the source of the efflux and determine its accumulated effect at various locations near the thruster. Comparisons of in situ and ex situ transmittance measurements of samples exposed to thruster efflux are also presented.

Introduction

Knowledge of the sputtered efflux distribution resulting from operating mercury Hg ion thrusters can be useful to the spacecraft designer. Of particular interest is the condensible efflux which can form as a result of (1) impingement of beam ions on thruster grids, (2) impingement of charge exchange ions on accelerator grids, (3) sputter erosion of discharge chamber components, and (4) impingement of mercury ions on neutralizer components. The resulting metallic efflux if allowed to deposit as thin films on spacecraft surfaces could change the optical properties of optical instruments, solar panels, and thermal control coatings. The sputtered efflux pattern must be considered in spacecraft design to prevent degradation of critical surfaces. This consideration requires quantitative knowledge of the condensible sputtered efflux for the primary or auxiliary propulsion ion thruster being considered.

The present study was undertaken to investigate the sputtered efflux from 5-, 8-, and 30-cm diameter Hg ion thrusters. An attempt was made to determine the sources of sputtered material and the efflux distribution. The results were accomplished by using solar cell cover slides which were positioned at various locations near each thruster. The thrusters were operated at fixed operating conditions for durations ranging from several hours to 7500 hours. After each test the spectral transmittance of each sample was determined and compared with the initial spectral transmittance. These data can be used to determine the accumulative effect of the sputtered material on spacecraft surfaces. The samples were then spectrographically analyzed to identify the sputtered elements to aid in determining the source of sputtered efflux.

A quartz crystal microbalance (QCM) was used to determine the film thickness and the rate of sputtered efflux (flux) at various locations near each thruster. The sample total transmittance data was correlated to the QCM data to generate a relation between total transmittance and sputtered film thickness. These data along with sputtered efflux data obtained from different thrusters operating at various conditions are presented herein.

Apparatus and Procedure

Detectors

Fused silica solar cell cover plates can be used to measure sputtered efflux from mercury ion thrusters. (1) The plate samples, 2.1 cm x 2.0 cm x 0.15 cm, were placed inside slotted stainless steel boxes, (fig. 1) to minimize tank wall, tank baffle, and support structure back sputter, and positioned at desired locations near the thruster. A datum point consisted of operating each thruster at a constant operating condition for a given amount of time during which sputtered material from thruster components deposited on the samples. After the test the samples were removed, and the spectral transmittance between 0.398 μm and 2.16 μm was measured using an integrating sphere-monochromator. (2) (The spectral transmittance is the ratio of a photodetector signal activated by a light source which passes through a sample to that with no sample.) Using the Johnson curve of solar spectral irradiance (3), a technique was employed that divided the solar spectrum into 2% energy increments to obtain discrete spectral transmittance data points. (2) The integration of the spectral transmittance data points gave the total transmittance. Comparison of spectral data before and after efflux exposure can be used to determine quantitatively the optical effects of sputtered thruster material on the operation of solar cells, thermal control coatings, optical windows, or any other device sensitive to this wavelength region.

The film depositions on the fused silica samples were then spectrographically analyzed using a standard arc emission technique to determine film composition. This information along with the location and view factor of each sample enabled the source of sputtered material to be determined. The film theoretical density could also be determined from the results of the spectrographic analysis.

Quartz crystal microbalances (QCM's) were used to measure sputtered flux. The resonant frequency of piezoelectric quartz crystals were a function of deposited film thickness and its density. (4) A 5 MHz cut crystal was used for all tests. If the density of the deposited film is assumed to be the theoretical density, a simple calculation yields the film thickness. The linear relationship is given in Eq. 1.

$$\Delta t = C_f \, \Delta f / \rho \qquad (1)$$

where

Δt = change in film thickness, Å

C_f = mass sensitivity constant of 5 MHz quartz crystal = 1.8 gm/cm^2/cycle/sec

Δf = change in quartz frequency, Hz

ρ = density of deposited material, gm/cm^2 (10.2 gm/cm^3 for all data reported since molybdenum was the major constituent)

The quartz frequency was monitored and recorded with the thruster run time so that a time rate of deposition could be determined.

5-cm Diameter Ion Thrusters

A 5-cm diameter ion thruster (SIT-5) with an electrostatic vector grid [5] was endurance tested for 7500 hours. [6,7] The components that could contribute as major sources of sputtered efflux were thought to be the ground screen, accelerator grid, and neutralizer. Figure 2 shows the thruster with the relative locations of these components in addition to the placement of sputtered efflux samples. The neutralizer keeper cap was located 3.2 cm downstream of the accelerator grid and 3.2 cm radially from the edge hole of the accelerator grid. Beam profile data of the SIT-5 indicated that the neutralizer keeper cap could be subjected to moderate sputter erosion. [5] The ground screen was designed so that it was 0.5 cm downstream of the accelerator grid at a radial distance of 3.2 cm from the edge hole of the acceleraotr grid to prevent direct Hg ion impingement.

Two fused silica sample plates were used to measure the sputtered flux from the thruster. Figure 2 shows their location to be approximately in the plane of the accelerator grid. Sample 1 had a view factor that included the accelerator grid. Sample 2 could detect sputtered material from the neutralizer as well as the accelerator grid.

Sputtered flux emanating from the thruster was measured for another SIT-5 thruster with electrostatic-vector accelerator grid. This thruster was being tested to determine the effects of discharge voltage ΔV_I on internal thruster component sputtering and the effects of the corresponding accelerator drain current Ja on external efflux. The results of the internal sputtering investigation was reported in Ref. 8. The accelerator drain current was 130, 90, and 80 microamperes,(μA) for the three tests in which ΔV_I was 36.6, 39.6, and 42.6 volts, (V), respectively. All other thruster conditions were maintained at nominal 5-cm diameter thruster values during each 400 hour test. [8] Fused silica samples and QCM's were used to measure sputtered flux. Each sample box was positioned so the samples and the thruster axis defined a horizontal plane (fig. 3). The samples were located in the same positions for all three tests. Each sample was located 42 cm from the center of the accelerator grid. The angle (α) between the thruster axis and each sample was varied from 35° to 90°. The samples and QCM's were arranged to determine the angular sputtered flux distribution.

8-cm Diameter Thruster

The sputtered flux from an 8-cm diameter thruster using dished extraction grids (0.25-cm dish depth) was determined while the thruster was being cyclic endurance tested. [9] Fused silica samples or microscope glass slides along with a QCM were mounted on a moveable rod that was parallel to the thruster axis (fig. 4). A gate valve was used to remove the rod and detectors while the thruster was off. All samples were positioned at the same perpendicular radial location (12.5 cm) from the thruster axis but at different axial (z) distances (parallel to the thruster axis) from the accelerator grid. The locations in the z direction varied from -1.5 cm (upstream of the accelerator grid) to 5.7 cm downstream of the accelerator grid.

30-cm Diameter Thruster

Efflux measurements on a 30-cm diameter thruster were made in a similar manner to those for 5-cm and 8-cm diameter thrusters. A modified 400 series thruster [10] was operated at various conditions both with and without compensated dished grids. The thruster operation was scheduled for tests other than efflux sample experiments. Hence each thruster test was operated at different conditions. Initially 6 fused silica samples were placed 15° apart on a curved rod with a radius of curvature of 30 cm. The center of the arc was located at the edge apperature of the accelerator grid. All samples faced the center of the accelerator grid, and their locations ranged from 15° to 90° with respect to the thruster axis. This sample arrangement was used only once because the sample boxes at 15°, 30°, and 45° were sputter eroded by the ion beam. To overcome this problem, two curved rods were used to mount the sample boxes. One rod had a radius of curvature of 30 cm and the other, 60 cm. Both curves had their center at an edge apperature of the accelerator grid. The sample boxes were attached to each rod at 90°, 75° and 60° with respect to the thruster axis. The azimuthal angle (β) that the rods make with respect to the line joining the neutralizer and accelerator grid centerline was varied between 0° and 180° in steps of 90°. For each datum point the rods were positioned so that no sample view factor included the other support rod. A sketch of this arrangement is shown in Fig. 5.

Vacuum Facility and Facility Backsputter

Three different vacuum facilities were used to obtain sputtered efflux data from Hg ion thrusters. One of the tanks, shown in Fig. 6, was considered ideal for efflux measurements. It contained a frozen Hg target to minimize condensible material from being sputtered from the target. [6] This facility (tank 5 N) was used for the 5- and 8- cm diameter thruster endurance tests. A gate valve was added prior to the 8-cm diameter thruster test to enable the samples and QCM's to be removed and repositioned when desired. Fused silica samples that faced either the tank walls or the frozen Hg target were used to estimate back sputtered tank or target material. These back sputter samples were not enclosed in shielded boxes (fig. 4).

Short term (400 hours) 5-cm diameter thruster tests were run in tank 1, a 1.5 m diameter by 3 m long tank shown in Fig. 7. The thruster and efflux apparatus were contained in the 1 m diameter bell jar of this tank. Backsputter samples were placed in the plane of the accelerator grid and in the plane of the thruster backplate. The samples faced the tank target at both locations.

Figure 8 shows the large 7.6 m diameter tank

(tank 6) which was used for 30-cm diameter thruster efflux tests. The tests were run with the thruster mounted in the 3 m diameter port. Other thrusters and experiments were operated in this facility simultaneously. (11) This mode of operation resulted in excessive efflux material in the tank and this phenomenum has been noted in Ref. 12. As for tank 5N samples were positioned to view the backsputter from the tank walls.

In Situ spectral Transmittance Measurements

To evaluate the optical effects of exposing the sputtered efflux to air and to verify the validity of the spectral transmittance measurements made ex situ in an integrating sphere, an experiment was undertaken to make in situ spectral transmittance measurements. The experimental apparatus is shown in Fig. 9. A SIT-5 thruster with electrostatic accelerator grid was used in the 1 m diameter port of tank 1. A light source was placed in front of an 18 cm diameter side port. A slotted chamber in front of the light source was used for inserting neutral density narrow band pass filters. A 4 mm x 4 mm active area end-on pencil thermopile was placed inside a diametrically opposite side port. A fused silica sample was mounted in front of the thermopile on a lever arm so that it could be rotated. The thruster was operated at fixed thruster conditions for 150 hours. After 150 hours with the thruster off and with the facility still evacuated, the transmittance (thermopile response with sample in front of thermopile to that with no sample) of the efflux coated sample was determined with each filter. The data points were taken within 6 hours after the thruster was shut down. The test chamber was bled up with air to atmospheric pressure and then evacuated to 5×10^{-4} torr at which time the spectral transmittance was taken again.

Results and Discussion

In Situ Spectral Transmittance

Since all ex situ spectral transmittance data reported herein were made in an integrating sphere, the thin film which was sputter deposited in a vacuum chamber was exposed to air before the transmittance data was taken. In situ spectral transmittance data were obtained to verify the ex situ integrating sphere data. The results of the in situ measurements are shown in Fig. 10. For the efflux sputtered from thrusters the spectral transmittance increased at short wavelengths after exposure to air. The oxygen apparently combined with molybdenum (major constituent) to form a molybdenum oxide which reduced the thickness of the free metal portion of the film, thus increasing the spectral transmittance. (13) The effect was neglibible at wavelengths larger than 4660 Å (filter peak wavelenght), but at wavelengths less than 4660 Å the effect (greater transmittance) increased as the wavelength decreased. At 4000 Å the transmittance nearly doubled. However, the effect on the total transmittance was only a 3% increase for the very thin film (probably less than 20 Å) tested. If a thicker film were evaluated for oxidation effects, the effect on total transmittance would be less than 3%. The spectral transmittance measurements made in the integrating sphere were valid representations of the effects of sputtered efflux from ion thrusters at wavelengths longer than 4660 Å, and for all the data presented herein the oxidation effects of the sputtered films on transmittance data was neglected.

Facility Backsputter

Fused silica samples were positioned in each tank to determine the amount of backsputter from tank walls and downstream targets. The backsputter samples that faced the downstream target in tank 1 (fig. 3) revealed only trance amounts of ion when spectrographically analyzed. These results indicated that materials sputtered from tank walls and target could be neglected. Therefore, for 5-cm diameter thruster tests this facility was quite adequate.

A sample (not enclosed in a shielded box) that faced the tank side wall for over 200 hours of thruster operating time in tank 5N received no optically detectable backsputtered material. However, spectrographic analysis of samples which viewed the frozen target indicated that trace amounts of molybdenum, iron, and/or mercury were deposited depending on the sample location with respect to the accelerator grid plane. It was essential that the samples in this facility were placed in shielded holders to minimize the effect of backsputter. Facility designs with frozen Hg targets did not totally prevent facility backsputter.

Large amounts of iron, nickel, copper, and other tank materials were detected by backsputter samples from tank 6. The backsputter is partially due to the high beam current of the 30-cm thruster, the simultaneous operation of several thrusters and experiments, and the highly contaminated tank walls. Extreme precaution had to be taken to insure the integrity of efflux measurements made in this tank. The best means of protecting the samples was to put them into shielded boxes. The boxes limited the view factor of the sample to include only certain thruster components, and they protected the samples from tank backsputter.

Film Thickness and Transmittance Correlation

To measure the thickness of a thin film sputtered from a thruster and to determine its spectral characteristics, QCM's and fused silica samples were interchanged at same location 2 cm downstream of the accelerator grid of an 8-cm diameter thruster. The thruster was cyclic operated at the same conditions for each test. Shown in Fig. 11 is the sputtered deposition rate measured by a QCM. The amount of condensible material emanating from the thruster is a linear function of time, and in this location the rate was 5.3 Å/hour. A spectrographic analysis of the deposits on QCM's and fused silica samples indicated that all the films were composed of molybdenum as the major constituent and tantalum, mercury and/or iron as minor constituents. This composition was evident for most samples as shown in Table I. In general the amounts of each element increased as the test duration increased.

Shown in Fig. 12 is the spectral transmittance of micorscope cover slides placed 2 cm downstream of the accelerator grid for various lengths of time (5, 21, 46, 69, 96, 162 hours). The film thicknesses of each deposition which was determined from QCM data is also given in Fig. 12. This value of film thickness may not be the true optical thick-

ness since the sticking coefficients of the QCM and microscope cover slides probably were not the same. (14) For short periods of time (~50 hours) or small thicknesses, there is a rapid reduction in transmittance at all wavelengths. The changes in spectral transmittance due to increased film thickness, however, are wavelength dependent, the largest reductions in transmittance occurring at short wavelengths. This trend can be seen more clearly in Fig. 13 where the data presented in Fig. 12 is replotted for wavelengths of 4500 Å, 8200 Å, and 15,000 Å. For any time exposure the transmittance at 4500 Å is less than the transmittance at 8200 Å which in turn is less than that for 15,000 Å. From Fig. 13 it is evident that although the deposition rate of the film as measured by the QCM is almost linear with time (fig. 11) the reduction in spectral transmittance is not linear with time. Figure 14 shows that the total transmittance is also not linear with time.

In figure 12 for thicknesses of 27 Å and larger, the reductions in spectral transmittance were uniform with increasing film thickness and did not contain unusual absorption patterns. This uniformity in reduction may be due to the fact that the material was deposited at very slow rates. Sennett and Scott have observed similar results for silver films. (15) For films less than 27 Å thick, there was not a uniform reduction in transmittance at a given wavelength. Instead for each test absorption bands would shift from one wavelenght region to another. However, for films greater than 27 Å thick, the data presented in Fig. 12 were typical of the spectral transmittance data obtained from the efflux measurements of molybdenum, tantalum mercury and/or iron composition. The data were reproducible for these elements and these thicknesses. The total transmittance of the films could be plotted as a function of film thickness because the spectral transmittance was inversely proportional to the film thickness at all wavelengths. This plot is shown in Fig. 15 in which the total transmittance is plotted as a function of the logarithm of film thickness. The total transmittance decreased uniformly as the film thickness increased and became negligible at a film thickness of about 1000 Å. Thus for a film composed mainly of molybdenum at least 27 Å thick, the total transmittance could be used to determine the thickness of the deposition.

The nature of the total transmittance allowed spectral transmittance curves in Fig. 12 to be used to calculate reductions in performance of solar cells, thermal control coatings, or optical devises. (1) Care should be taken in evaluating the effects of a deposit of efflux at a given location near a thruster if the total thickness of a film is less than 27 Å, if the rate of deposit was of order Å/sec instead of Å/hour, or if the composition of the film differed from the Mo, Fe, Hg, and/or Ta composition found in these tests. A QCM used to measure the sputtered flux without spectral information might yield insufficient information to allow proper evaluation of the effects of efflux on spacecraft surfaces or components.

5-cm Diameter Thruster

Because every efflux deposition was similar in that each had molybdenum as the major constituent, the total transmittance of the thin films will be used to discuss the results of the 5-cm diameter thruster. The spatial distribution of sputtered efflux as indicated by the transmittance of the deposited films is shown in Fig. 16(a). For the three thruster conditions investigated the results showed that as the angle (α) between the thruster axis and sample location decreased from 62° to 50° the sputter efflux increased. At angles less than 50° (probably close to 45°) ion sputter erosion of the samples exceeded the sputtered deposition. The net result was erosion of the clean fused silica by ions as depicted by data at $\alpha = 35°$. By using Fig. 16(b) these results could be qualitatively explained. The ion beam profile is approximately a gaussian distribution while the sputtered efflux profile is theoretically a cosine distribution. The ion sputtering rate equalled the sputtered flux at approximately 45°. At angles greater than 45° the cosine distribution of sputtered efflux was larger in magnitude which would cause more material to be deposited than sputtered. At angles less than 45° the gaussian distribution dominated, and the results was ion sputtering of the sample.

The sputtered efflux showed a dependence on Ja as shown in Fig. 16(a). A higher Ja resulted in a larger sputtered efflux which in turn resulted in a lower transmittance. At 62° with respect to the thruster axis the sputtered efflux increased by 40% as Ja went from 80 to 130 μA. The efflux thickness of Fig. 16(a) was determined by measuring total transmittance of each sample and converting to film thickness using figure 15. Because the samples located at 35° to the thruster axis were in the ion beam, the film thicknesses were most likely negligible. Visual inspection indicated the sample had been eroded. Transmittance data revealed a lower transmittance after the tests, and the data points at 35° with respect to the thruster axis are estimates of film thickness that corresponded to the reduction in total transmittance.

Sputtered efflux data obtained from three different tests in which a 5-cm diameter thruster was operated at nearly indentical conditions is shown in Fig. 17 as a function of angle from the thruster axis. The solid curves were the anticipated sputtered flux for three different Ja's of 80, 90, and 130 μm. These results were calculated from the cosine distribution analysis of sputter yield due to charge exchange ions (group 3, Ref. 16) from Ref. 17. The dotted line indicated the measured sputtered efflux. The difference between the theoretical curve and experimental results at angles less than 58° represented the amount of material resputtered by ions. The anticipated deposits which have a cosine distribution indicated that at 90° from the thruster axis the sputtered efflux from charge exchange ions would be zero. However, measurements of the sputtered efflux indicated a rate of about 0.035 Å/hour was being deposited. The detection of sputtered efflux at 90° could be the result of (1) the sputtered efflux from group 3 ions not following a cosine distribution, (2) the samples having a finite view factor, (3) the accelerator grid hole walls having a finite axial length, or (4) the possibility of second bounce of sputtered material. Further investigation is needed to determine if condensible efflux existed beyond 90°.

8-cm Diameter Thruster

The sputtered flux data from an 8-cm diameter thruster with 0.25-mm dished extraction grids was measured with a QCM for various distances upstream and downstream of the accelerator grid plane at a fixed perpendicular distance of 12.5 cm from the thruster axis. Figure 18 shows the dependence of sputtered flux on test duration for a fixed QCM location. The sputtered flux decreased as the test duration increased and appeared to approach an asymptote. A similar decrease in sputtered flux has been previously observed [9] and was probably due to time dependent direct ion impingement of some accelerator grid edge aperatures. The accelerator holes changed dimension slowly until the configuration is optimized for thruster operating conditions.

Figure 19 shows the spatial net efflux distribution for an 8-cm-diameter thruster. The maximum measured sputtered efflux occurred at 2 cm downstream of the accelerator grid plane (77° from thruster axis). The spatial efflux distribution did not follow a cosine distribution. Instead there was more efflux than predicted by a cosine distribution at large angles with respect to the thruster axis. The net flux dropped abruptly to zero at approximately 5.5-cm downstream of the accelerator grid plane. At this location the ion sputtering as indicated by QCM readings equalled the sputtered flux and defined an erosion-deposition equilibrium condition at 57° from the thruster axis.

At angles greater than 90° a sputtered flux of about 0.2 Å/hr was measured. The pattern of the film on the samples at these locations upstream of the accelerator grid plane indicated that the material was coming through the perforated ground screen. Spectrographic analysis revealed that the deposition was mainly molybdenum which indicated that the sputtered efflux was from the accelerator grid. An explanation for this observation was that the grid material was sputtered toward the underside of the ground screen. Because the sticking coefficient of stainless steel was not unity, some of the efflux would bounce off the ground screen. This efflux would then emanate in directions that would result in molybdenum depositions that were greater than 90° from the thruster axis. A nonperforated ground screen would prevent any upstream flow of multiple bounce sputtered molybdenum. This film inside the ground screen even after 10,000 hours, would only be 250 Å and flaking would not be a serious problem.

30-cm Diameter Thruster

In Fig. 20 is presented the ratio of the final to initial total transmittance for six fused silica samples exposed to the efflux from a 30-cm diameter thruster with compensated dished grids. The thruster was operated at a beam current of 2 amperes, (A) for 43 hours. The sample holders located at 15°, 30°, and 45° showed signs of being eroded by the ion beam. All of the front surfaces of the boxes at 15° and 30° and half of the front surface of the box at 45° were cleaned by the ion beam. The front surfaces of the boxes at 60°, 75°, and 90° looked unchanged. This observation meant that there was sufficient ion beam divergence to cause noticeable sputtered erosion of the sample holders even at 45° with respect to the thruster axis.

Even though the sample at 15° was eroded by the ion beam, the total transmittance of the sample did not change. The only effect of the ion beam was to change the transmittance through the sample from specular to diffuse. The maximum reduction in transmittance of a sample occurred at 45°, and as the angle increased the transmittance increased. The sample at 90° suffered a reduction in transmittance which indicated sputtered material was deposited on the sample. This sample at an azimuthal angle of 180° had a view factor of the neutralizer. Spectrographic analysis of the deposited film indicated that Ta, of which the neutralizer keeper cap and heater shield was composed was being deposited on the sample as the major constituent. The neutralizer was located 45° from the thruster axis. The other samples had a major constituent of molybdenum implicating the grids as the major sputter source. Ta, Fe, and Hg were also found in trace amounts on the samples.

The solid curve shown in Fig. 21 is the sputtered flux of condensibles as calculated from a cosine distribution analysis of the sputter yield due to charge exchange ions from Ref. 17. Also shown in the figure are the data points shown in Fig. 20 converted from a total transmittance to a sputtered flux by using the total transmittance-film thickness relation (fig. 15). The measured flux was much less than the predicted flux but did not go to zero at 90°. As was the case for the 5- and 8-cm diameter thruster, the 30-cm diameter thruster efflux did not exactly follow a cosine distribution pattern. At 90° from the thruster axis there existed a measured flux of 0.1 Å/hour for this particular case. This measurement meant that the condensible efflux was composed of sources whose integrated total efflux distribution did not follow a spatial cosine distribution upon leaving the thruster.

Shown in Fig. 22 is the ratio of the final to initial total transmittance for samples located 30 cm from the accelerator grid at 60°, 75°, and 90° from the thruster axis and at an azimuthal angle of 180° plotted as a function of time. The data was taken during three separate thruster tests of 43, 107, and 289 hours with drain current values of 3.0, 2.6, and 3.5 mA, respectively. For the samples at 90° the reduction in transmittance was slower than for the samples located at 60° and 75°. Nevertheless all samples did suffer a reduction in transmittance. The samples at 90° had a view factor of the neutralizer and the major constituent of the deposited film was Ta. The samples located at 60° and 75° initially suffered a sharp decrease in transmittance. For the sample at 60° the transmittance was reduced to 0.26 of its initial value after 107 hours of testing.

In Fig. 23 is shown the results of exposing efflux samples at the same location, for the same length of time, and for two different thruster conditions. Operating the thruster at a lower discharge voltage caused the thruster to run at a lower propellant utilization efficiency. A lower propellant utilization efficiency increased the drain current which in turn increased the efflux. The samples received more efflux for ΔV_I = 33 V

and suffered a greater reduction in transmittance than the samples for ΔV_I = 37 V.

Samples were also placed near the thruster for tests at 90°, 75°, and 60° from the thruster axis, at various azimuthal angles and at distances of 30 cm and 60 cm from the thruster. These samples were exposed to different thruster operating conditions, different thruster components, such as baffles and grids, and various lengths of operating time. However, because of the variety of thruster operating conditions during the efflux measurements, it was not possible to generate an efflux function. In some thruster tests the operating conditions on the thruster were not held constant during a given sample exposure time. Also from test to test more than one variable was changing, making it impossible to correlate the efflux or a change in the efflux with any single parameter. Nevertheless, several comments on the data can be made. From spectrographic analysis of the samples, it was found that as the angle (α) decreases from 90° to 60° the amount of Hg and Mo found on the samples increases. Except for the azimuthal position of 180° and a sample angle (α) of 90° where Ta was the major constituent, Mo was the major constituent found on the samples. The Ta found on the samples was azimuthally directional, for changing the azimuthal angle, β, reduced the amount of Ta on the samples at a $\alpha = 90°$ location. At an azimuthal angle of 0° (above the neutralizer) no Ta was found in the $\alpha = 90°$ sample, which indicated that the neutralizer keeper and the heater shield were eroded by the ion beam.

Increasing the sample distance from the thruster at a given angle decreased the relative amount of material deposited on the samples. Shown in Fig. 24 is a plot of the ratio of final to initial transmittance as a function of angle from the thruster axis. Although the azimuthal angle (β) for the two distances was different the data does show that increasing the sample distance from the thruster at a given angle decreases the relative amount of material deposited on the samples. Using a set of dished uncompensated grids caused the largest reductions in transmittance of any sample ixposed for comparable lengths of time. Also placing an annular mask (25 cm I.D. and 30 cm O.D.) on the accelerator grid to block the outermost holes of the grids, did not decrease the material being sputtered, but actually increased it. The use of grid compensation [18] did change the erosion rate and may be a way of minimizing the amount of grid material being eroded.

Concluding Remarks

A technique has been developed which used spectral transmittance of samples exposed to thruster efflux to determine and characterize the effect of the efflux on spacecraft surfaces and optical devices. The ex situ transmittance measurements taken in an integrating sphere are representative of data taken in situ. An investigation of the backsputter from various facilities used for efflux studies revealed that caution must be taken to ensure that the efflux samples are protected from materials from tank walls and targets. One of the best ways to protect the samples was to put them inside small shielded boxes.

With few exceptions the composition of the sputter efflux deposited on the samples was molybdenum (major constituent) with trace amounts of tatalum, iron and/or mercury. Because deposited films had molybdenum as the major constituent, a relationship between efflux film thickness and total transmittance was established for film thicknesses between 30 Å and 1000 Å. It was then possible to determine the film thickness and its spectral characteristics from the total transmittance of the deposited efflux. Efflux samples could also be used as diagnostic tools to determine whether a thruster component, such as the neutralizer keeper cap, was being eroded.

The efflux from a 5-cm diameter thruster was deposited on samples located in the plane of the accelerator grid (an angle of 90° with respect to the thruster axis). An equilibrium between ion beam erosion and efflux deposition occurred between 45° and 60° with respect to the thruster axis. At angles greater than these the efflux deposition dominates and a deposition formed on the samples. At angles less than these the ion beam etched the samples causing the total transmittance to become diffuse rather than specular.

The 8-cm diameter thruster efflux results showed that the location of ion beam sputtering and efflux deposition equilibrium occurred at 57° with respect to the thruster axis. A small efflux was measured at $\alpha = 90°$ and the maximum efflux occurred at $\alpha = 77°$. The sputter flux decreased as the cyclic endurance test progressed and appeared to be approaching an asymptote.

The 30-cm diameter thruster had an ion beam erosion-efflux deposition equilibrium at 45°. The sputter flux was shown to be dependent on accelerator drain current. The neutralizer was positioned such that it was being sputtered by a small amount of direct ion impingement.

Refererences

1. Weigand, A. J., and Mirtich, M. J., "Change in Transmittance of Fused Silica as a Means of Detecting Material Sputtered from Components on a 5-cm Ion Thruster," TM X-68073, 1972, NASA.

2. Bowman, R. L., Mirtich, M. J., and Weigand, A. J., "Changes in Optical Properties of Various Transmitting Materials Due to Simulated Micrometeroid Exposure," presented at the Optical Society of America, Annual Meeting, Chicago, Illinois, Oct. 21-24, 1969.

3. Johnson, Francis S., The Solar Constant. Met Meteorol., Vol. 11, No. 6, Dec. 1954, pp. 431-439.

4. Wallace, D. A., "Use of Quartz Crystal Microbalance for Outgassing and Optical Contamination Measurements," Journal of Vacuum Science Technology, Vol. 9, No. 1, Jan. 1972, pp. 462-466.

5. King, H. J., Collett, C. R., and Schnelker, D. E., "Thrust Vectoring Systems. Part 1 - 5 cm Systems, "(Hughes Research Lab.; NASA CR-72877, 1970.

6. Nakanishi, S., and Finke, R. C., "A 2000-Hour

Durability Test of a 5-Centimeter-Diameter Mercury Bombardment Ion Thruster," TM X-68155, 1972, NASA.

7. Nakanishi, S., and Finke, R. C., "A 9700-Hour Durability Test of a Five Centimeter Diameter Ion Thruster," AIAA Paper 73-1111, Lake, Tahoe, Nev., 1973.

8. Power, J. L., "Sputter Erosion and Deposition in the Discharge Chamber of a Small Mercury Ion Thruster," AIAA Paper 73-1109, Lake, Tahoe, Nev., 1973.

9. Eight-cm Mercury Ion Thruster System Technology, AIAA Paper 74-1116, San Diego, Calif., 1974.

10. Rawlin, V. K., Performance of 30-cm Ion Thrusters with Dished Accelerator Grids, AIAA Paper 73-1053, Lake Tahoe, Nev., 1973.

11. Reynolds, T. W., and Richley, E. A., "Contamination of Spacecraft Surfaces Downstream of a Kaufman Thruster," TN D-7038, 1971, NASA.

12. Bechtel, R. T., Banks, B. A., and Reynolds, T. W., "Effect of Facility Backsputtered Material on Performance of Glass-Coated Accelerator Grids for Kaufman Thruster," AIAA Paper 71-156, New York, N.Y., 1971.

13. Hass, G., and Thun, L. E., eds., Physics of Thin Film, Vol. 4, Academic Press, 1967, pp. 37-41.

14. Langmuir, I., "The Evaporation, Condensation, and Reflection of Molecules and the Mechanism of Adsorption," The Collected Works of Irving Langmuir, Vol. 9 - Surface Phenomena, C. G. Suits, ed., Permagon Press, New York, 1961, pp. 42-68.

15. Sennett, R. S., and Scott, G. D., "The Structure of Evaporated Metal Films and Their Optical Properties," Journal of Optical Society of Amer., Vol. 40, No. 4, April 1950, pp. 203-211.

16. Staggs, J. F., Gula, W. F., and Kerslake, W. R., "Distribution of Neutral Atoms and Charge- Exchange Ions Downstream of an Ion Thruster," J. Spacecrafts and Rockets, Vol. 5, No. 2, Feb. 1968, pp. 159-164.

17. Kemp, R. F., Miller, W. D., Luedke, E. E., and Hall, D. F., "Effects of Electrostatic Rocket Material Deposited on Solar Cells," AIAA Paper 72-447, Bethesda, Md., 1972.

18. Rawlin, V. K., Banks, B. A., and Byers, D. C., "Design, Fabrication, and Operation of Dished Accelerator Grids on 30-cm Ion Thruster," AIAA Paper 72-486, Bethesda, Md., 1972.

Table I *Spectrographic results of sputtered material from* 8-cm diameter thruster for different test durations while operating in tank 5N. Samples located in plane of ground screen and had view factor of accelerator grid and neutralizer. Elements detected, Mg/cm^2.

Sample number	Test duration, hr	Film thickness, Å	Elements detected, Mg/cm^2			
			Fe	Hg	Mo	Ta
1	21	130	.38	.38	2.0	.24
2	48	280	.21	1.	4.3	.72
3	69	420	.28	1.	5.1	1.2
4	96	590	.3	2.	5.4	2.2
5	162	990	.4	.5	5.4	2.6

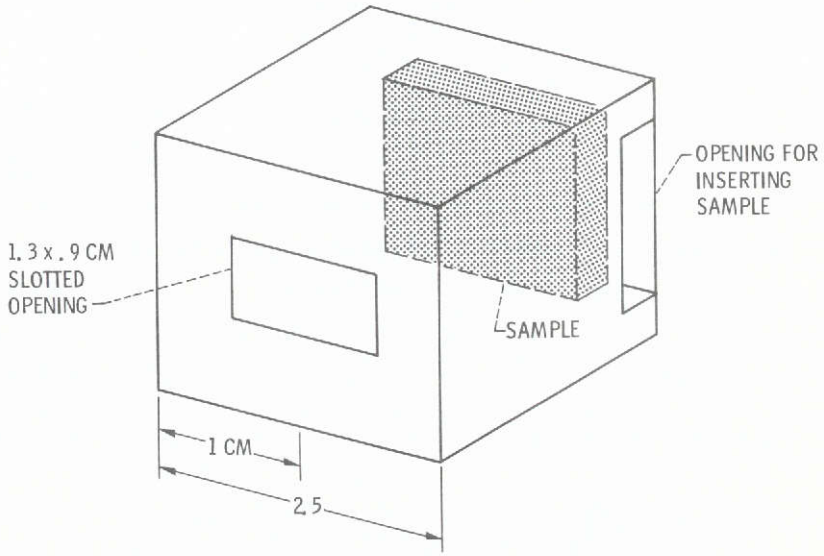

Figure 1. - 2.5 x 2.5 x 2.5 efflux sample box.

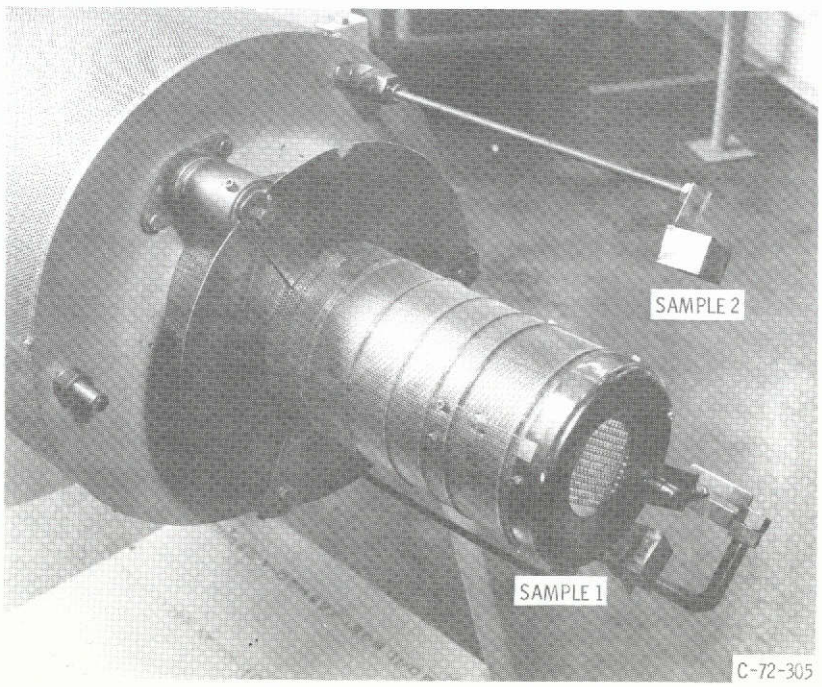

Figure 2. - Location of efflux samples for 7500-hour, 5-cm diameter thruster endurance test.

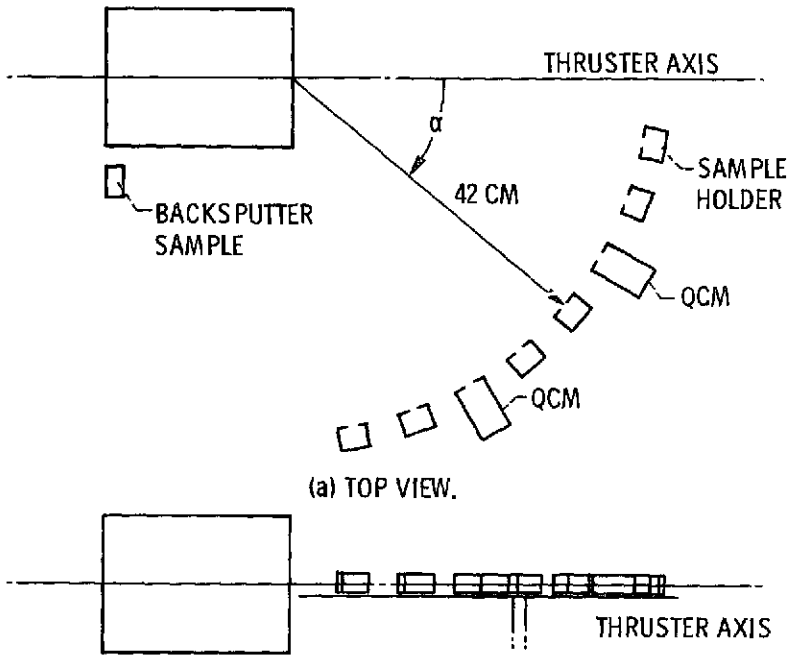

Figure 3. - Sample locations with respect to thruster axis for 5 cm diameter ion thruster ΔV_1 test.

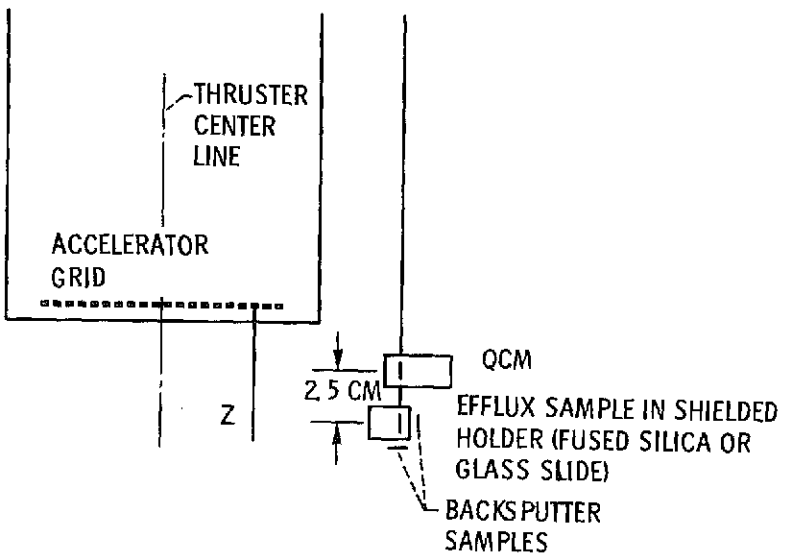

Figure 4. - Location of sample and QCM for 8-cm diameter thruster tests.

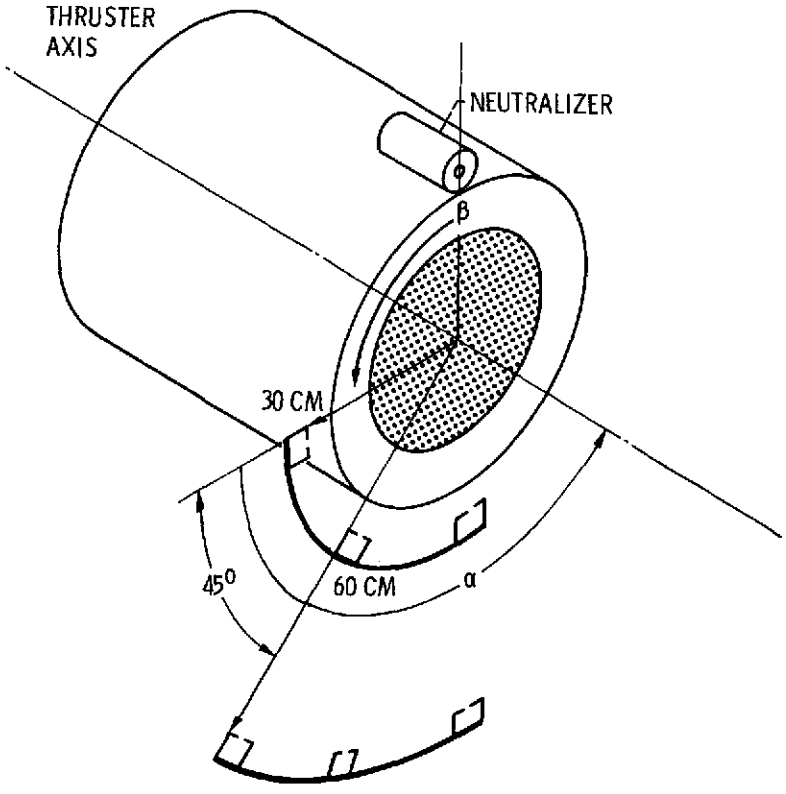

Figure 5. - Experimental setup for 30-cm diameter thruster efflux measurements.

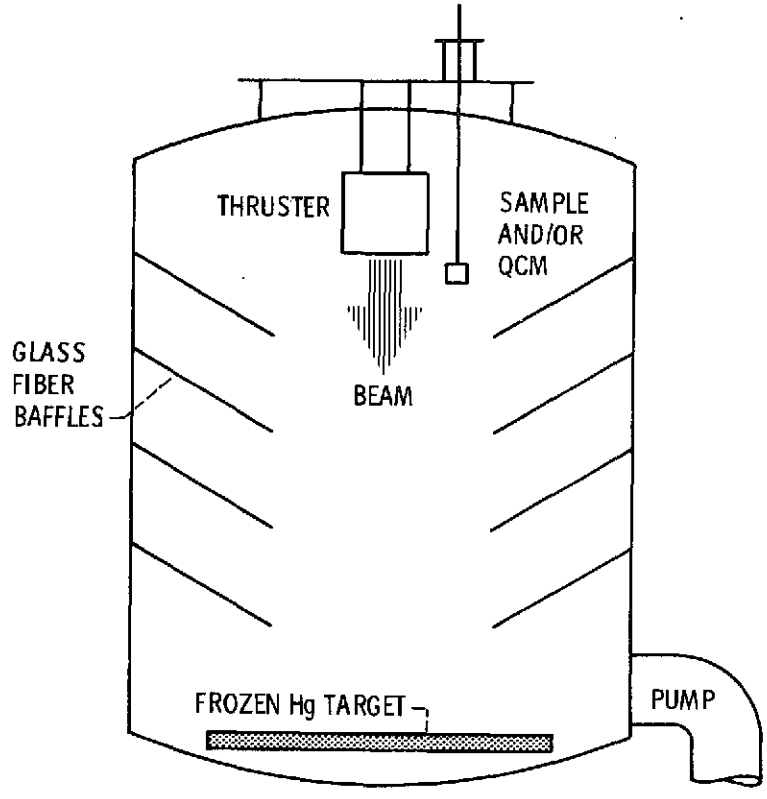

Figure 6. - Test facility (tank 5N) for 5- and 8-cm diameter thruster endurance tests.

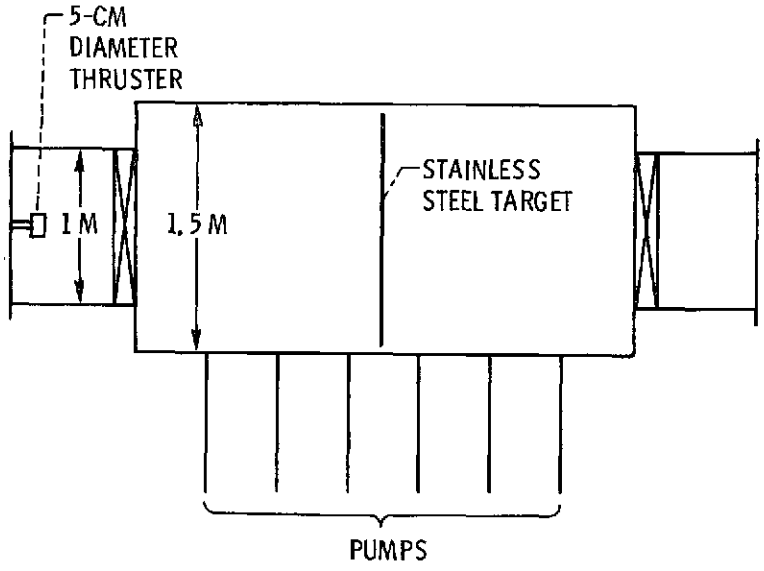

Figure 7. - 1.5 m diameter x 3 m test facility.

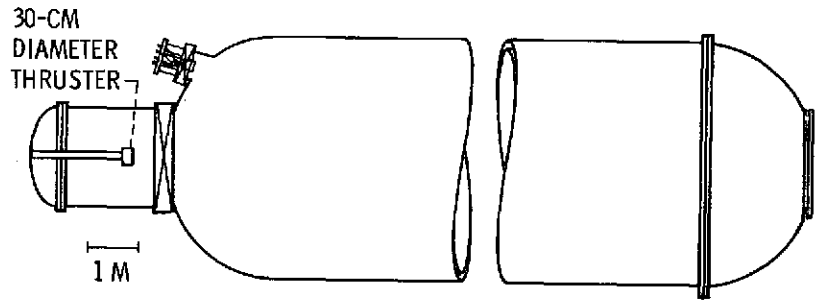

Figure 8. - 7.6 Diameter facility (tank 6) for 30-cm diameter thruster efflux tests.

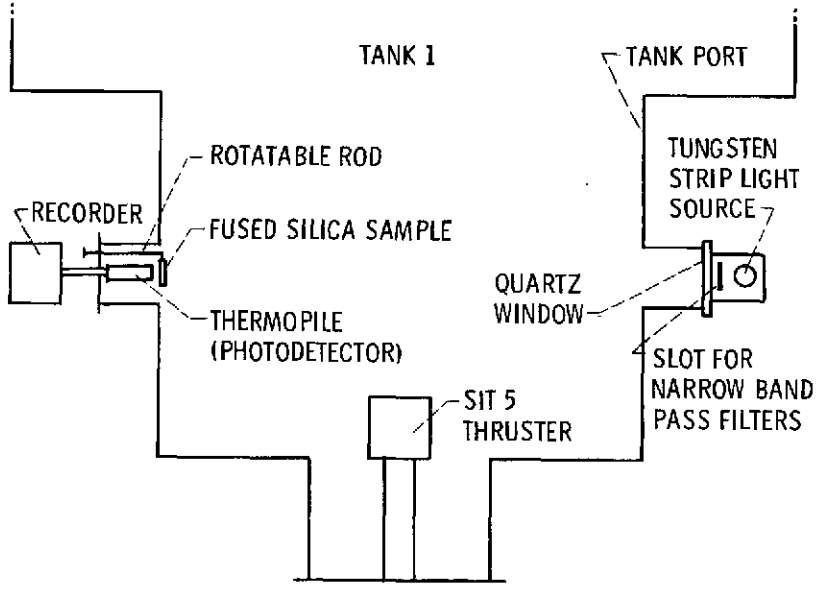

Figure 9. - Experimental apparatus for in situ spectral transmittance measurements.

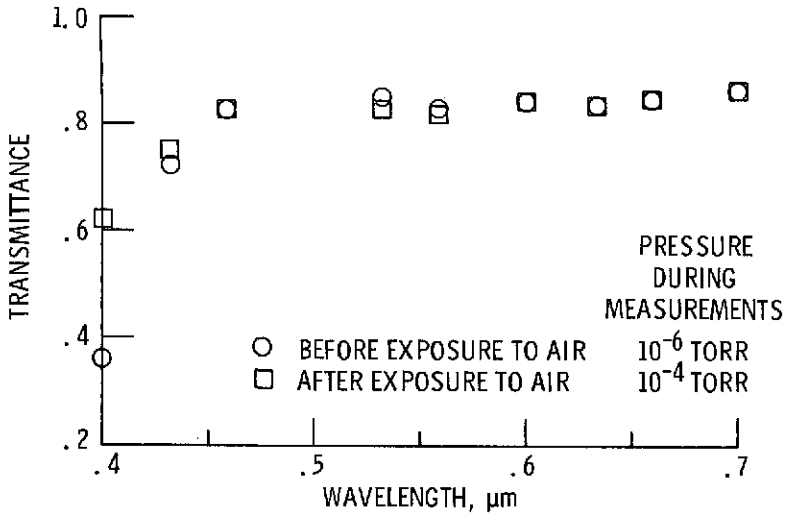

Figure 10. - Measurements of spectral transmittance before and after exposure to air.

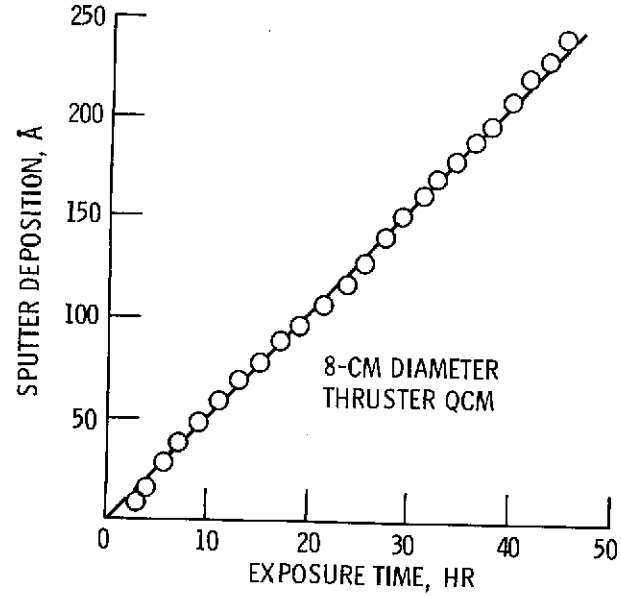

Figure 11. - Sputter efflux measured from 8-cm diameter thruster by QCM.

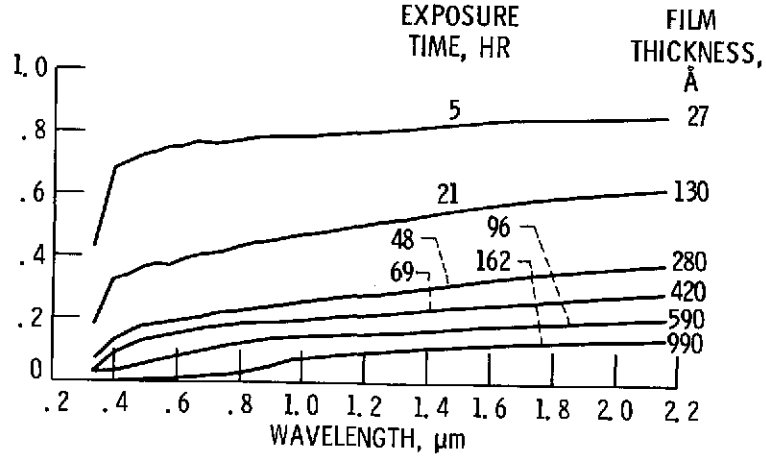

Figure 12. - Spectral transmittance of efflux samples located 12.5 cm perpendicularly from 8-cm diameter thruster axis. Sample location is 2 cm downstream of accelerator grid in a shielded box. Sample view factor is across accelerator grid.

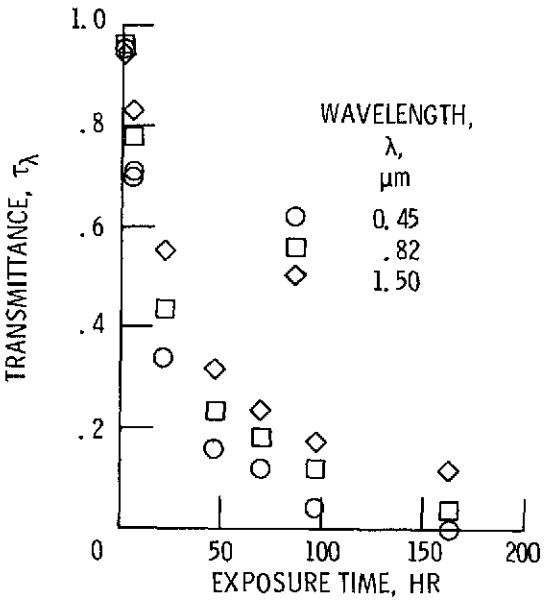

Figure 13. - Transmittance measurements as function of time for wavelengths of 4500 Å, 8200 Å, 15 000 Å. Data from efflux from 8-cm diameter thruster.

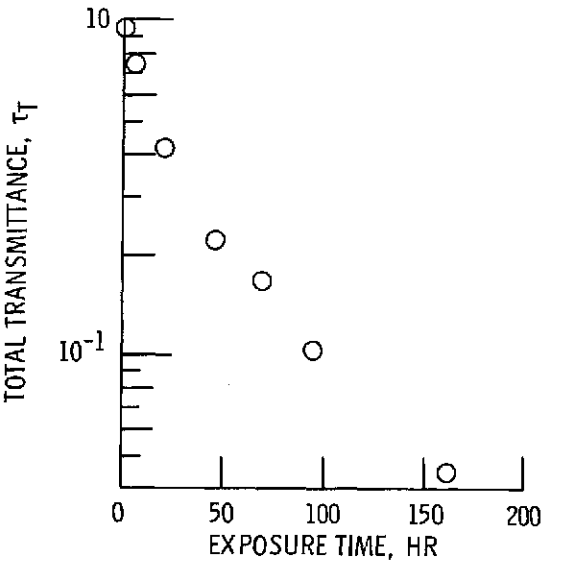

Figure 14. - Total transmittance of efflux depositions as function of exposure time with 8 cm diameter ion thruster. (Same samples as for fig. 12.)

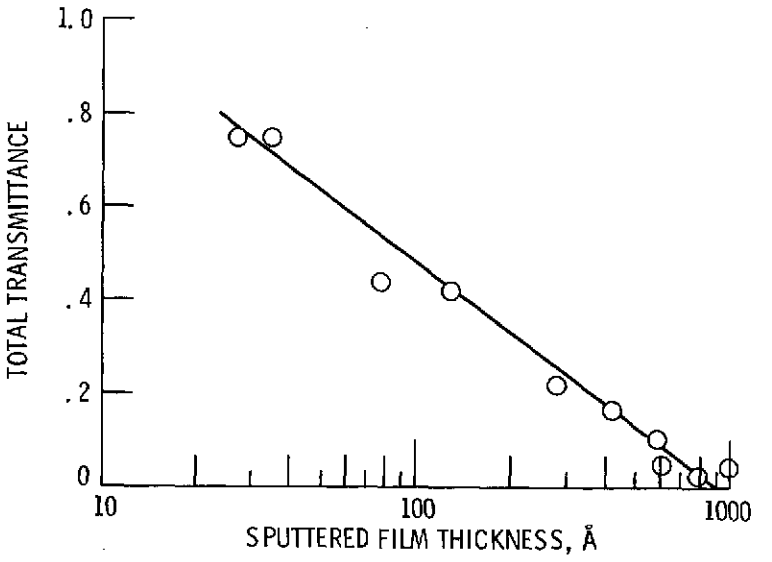

Figure 15. - Total transmittance of efflux samples as function of film thickness. Data from 8-cm diameter thruster. (Same samples as for fig. 12.)

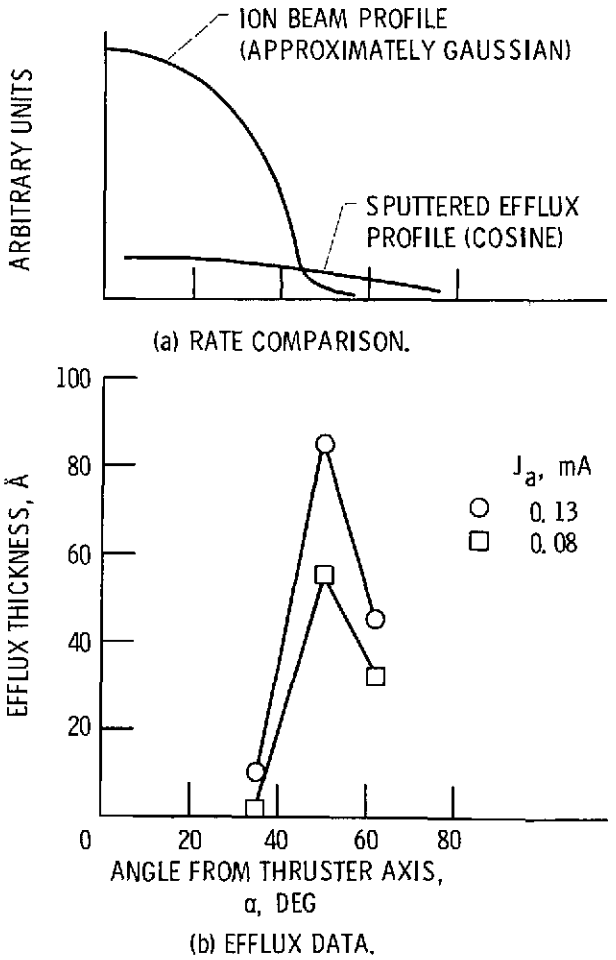

Figure 16. - Spatial distribution of sputtered efflux 42 cm from sit 5 thruster for J_a = 80 and 130 mA. Test duration, 400 hr.

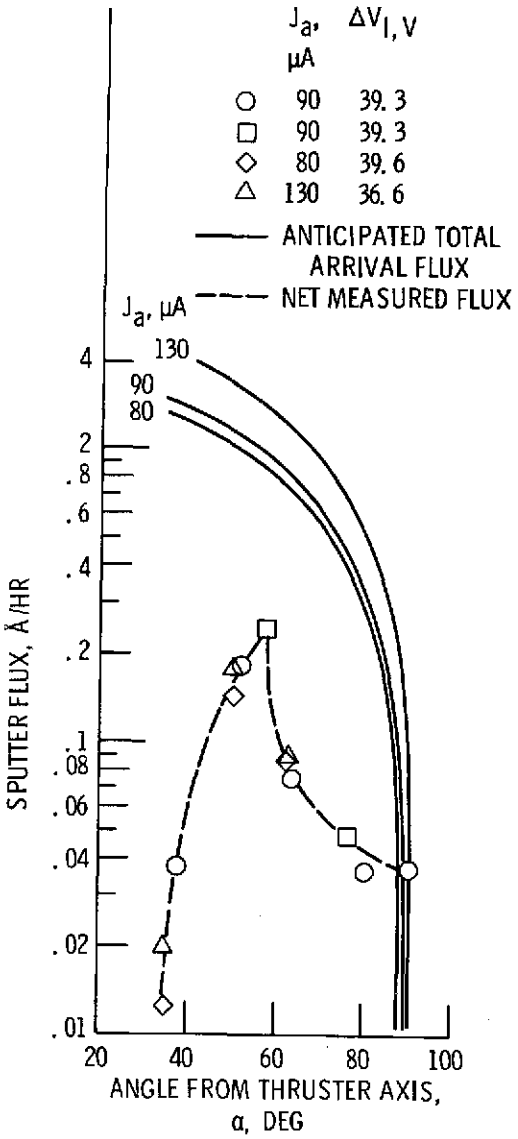

Figure 17. - Theoretical and experimental sputter flux as function of angle from thruster axis for 5-cm diameter thruster. All samples 42 cm from center of accelerator grid.

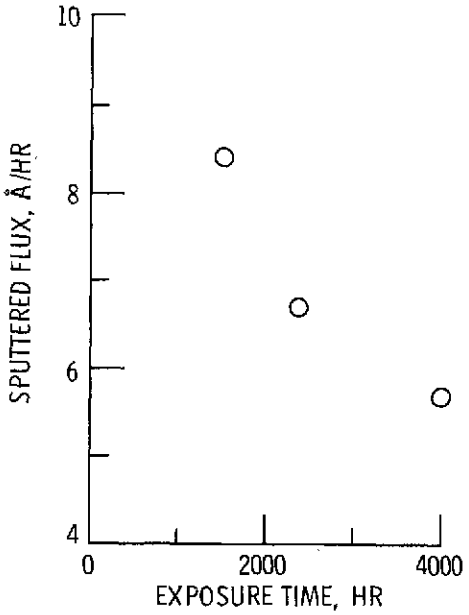

Figure 18. - Time variation of sputter flux for samples located at 2 cm downstream of accelerator grid plane for 8-cm diameter thruster.

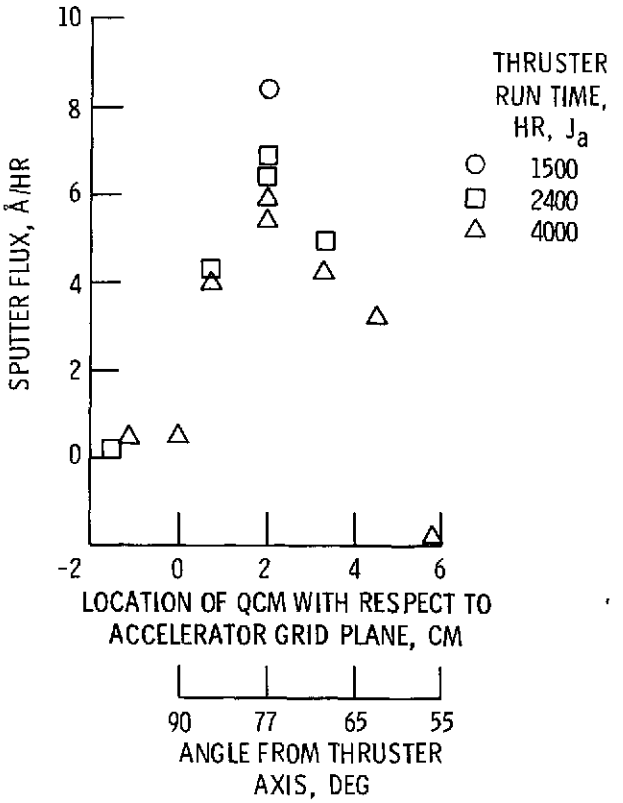

Figure 19. - Sputtered flux spatial distribution for 8-cm diameter thruster.

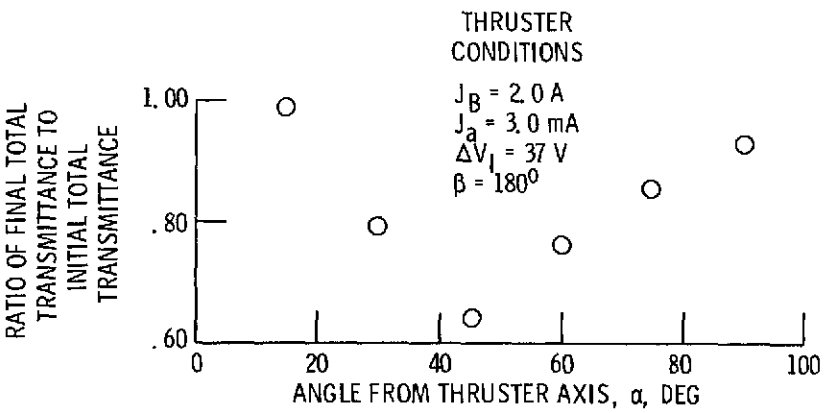

Figure 20. - Ratio of final to initial total transmittance of efflux samples located 30-cm from edge of accelerator grid of 30-cm diameter thruster.

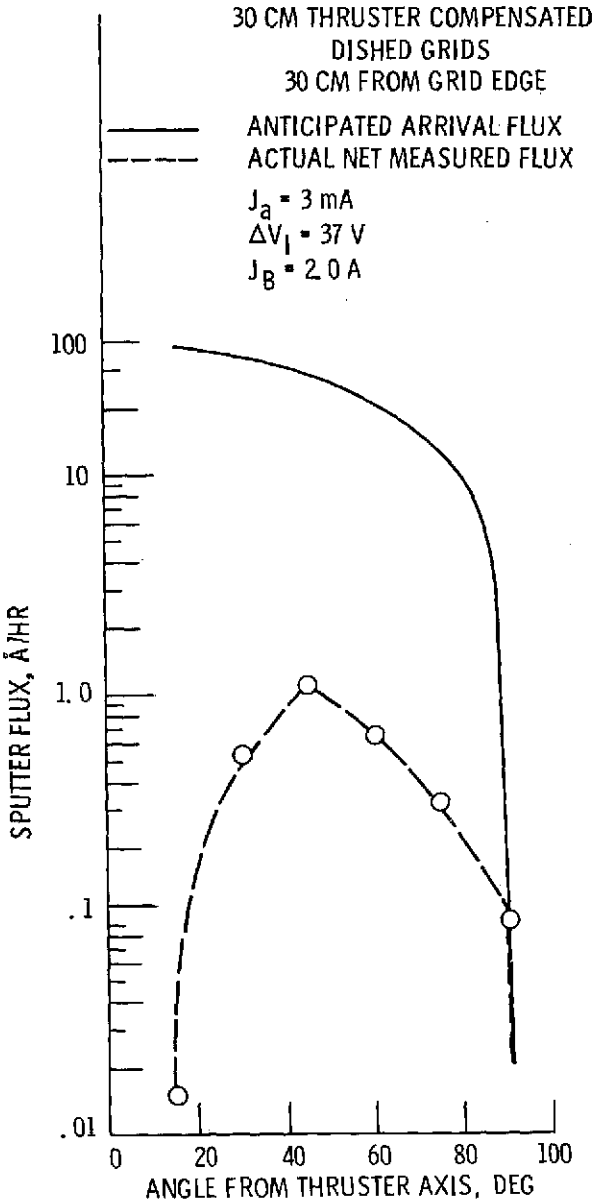

Figure 21. - Theoretical and experimental sputter flux as function of angle from thruster axis for 30-cm diameter thruster.

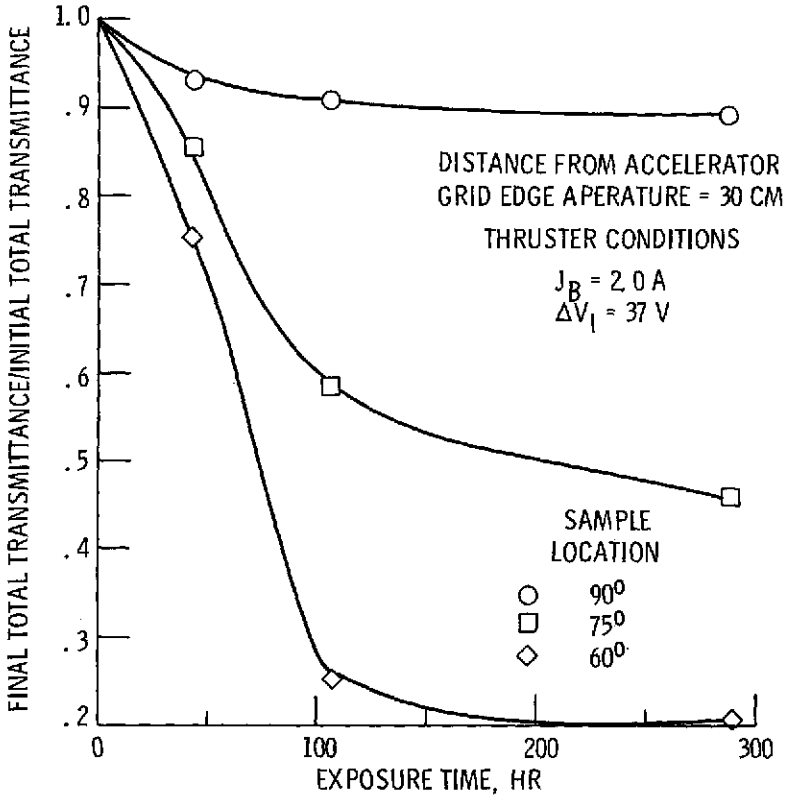

Figure 22. - Final to initial total transmittance ratio as function of thruster operation time for 30-cm diameter thruster.

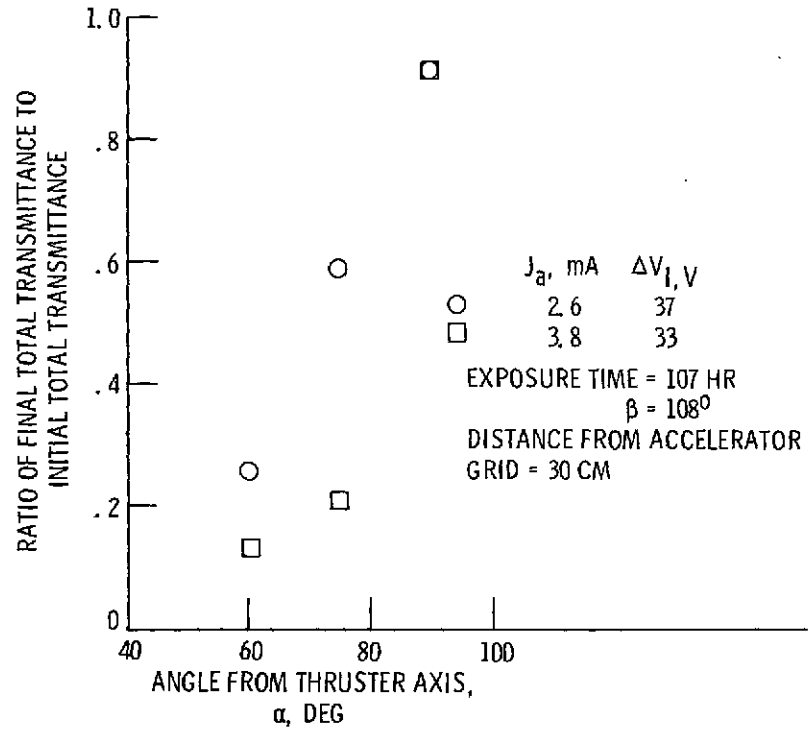

Figure 23. - Final to initial total transmittance ratio as function of angle from thruster axis for 30-cm diameter thruster.

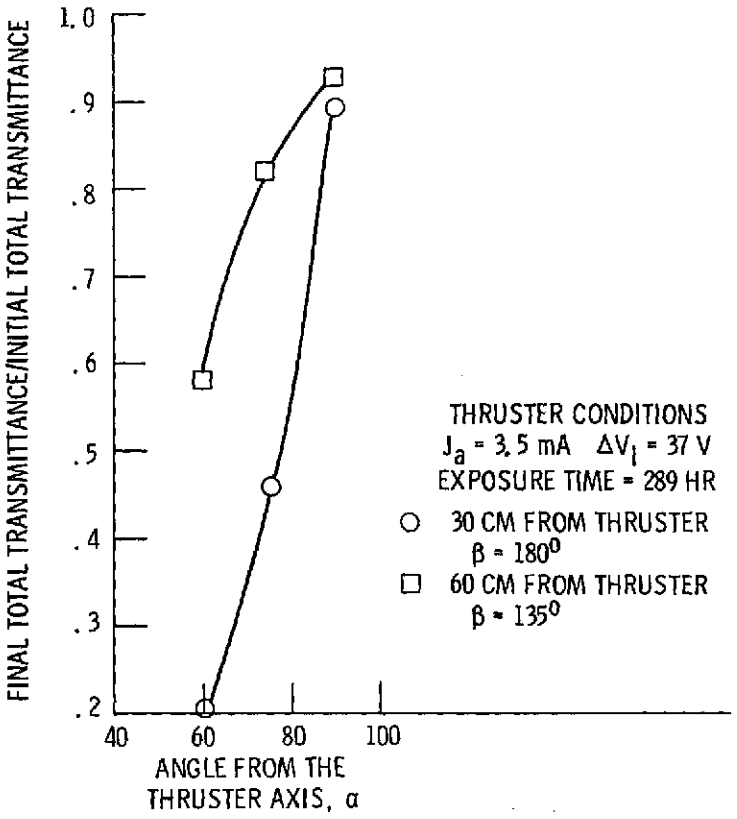

Figure 24. - Ratio of final total transmittance to initial total transmittance as function of angle from thruster axis for 30-cm-diameter thruster.